JACS
JOURNAL OF THE AMERICAN CHEMICAL SOCIETY
Communication
pubs.acs.org/JACS

Ultrafine Pt Nanoclusters Confined in a Calixarene-Based $\{Ni_{24}\}$ Coordination Cage for High-Efficient Hydrogen Evolution Reaction

Shentang Wang,[†,§] Xiaohui Gao,[‡,§] Xinxin Hang,[†,§] Xiaofei Zhu,[†] Haitao Han,[†,§] Wuping Liao,*[,†] and Wei Chen*[,‡]

[†]State Key Laboratory of Rare Earth Resource Utilization, Changchun Institute of Applied Chemistry, Chinese Academy of Sciences, Changchun 130022, China

[‡]State Key Laboratory of Electroanalytical Chemistry, Changchun Institute of Applied Chemistry, Chinese Academy of Sciences, Changchun 130022, China

[§]University of Chinese Academy of Sciences, Beijing 100049, China

Supporting Information

ABSTRACT: To obtain stable and ultrafine Pt nanoclusters, a trigonal prismatic coordination cage with the sulfur atoms on the edges was solvothermally synthesized to confine them. In the structure of $\{Ni_{24}(TC4A\text{-}SO_2)_6(TDC)_{12}(H_2O)_6\}$ ($H_4TC4A\text{-}SO_2$ = *p-tert*-butylsulfonylcalix[4]arene; H_2TDC = 2,5-thiophenedicarboxylic acid), three Ni_4-($TC4A\text{-}SO_2$) SBUs are bridged by three TDC ligands into a triangle and two such triangles are pillared by three pairs of TDC ligands to form a trigonal prism. The cage cavity has 12 sulfur atoms on the surface. Because of the porous structure and strong covalent interaction between metal and sulfur, ultrafine Pt nanoclusters composed of less than ~18 Pt atoms can be facilely confined in the present trigonal prismatic cage (**Pt@CIAC-121**). The as-synthesized Pt NCs exhibit higher electrocatalytic activity than commercial Pt/C toward hydrogen evolution reaction.

Polyhedral coordination cages (PCCs) or hollow metal−organic polyhedra with fascinating structures have broad potential applications.[1−3] Tunable pore sizes and controllable pore environments would facilitate the PCCs to act as functional molecular microreactors or to entrap various nanoparticles (NPs) to form nanomaterials with catalytic properties.[1a,c] Furthermore, the heteroatom donors on the framework would effectively prevent the aggregation and migration of catalytically active NPs in solid state, which consequently makes the NPs@metal−organic composite catalysts be highly active and reusable.[4] Calixarenes are reported to be a kind of effective multidentate ligands for the construction of PCCs.[5−8] For instance, a series of octahedral PCCs with tunable sizes were constructed by linking the M_4-TC4A or M_4-($TC4A\text{-}SO_2$) SBUs with deliberately chosen di/tricarboxylate ligands.[6,8a,b] A Johnson-type hexadecahedronal cage was constructed by linking M_4-TC4A SBUs with 5-(pyridin-4-yl)isophthalate.[7] Three trigonal prisms were assembled by two calixarene-capped $Na_2Ni_{12}Ln_2$ clusters and three linear dicarboxylates.[8c] All of these indicated that the shuttlecock-like M_4-calixarene SBU holds the desired curvature necessary for the construction of PCCs.

To fabricate some PCCs with heteroatom donors to bind Pt NCs, the M_4-($TC4A\text{-}SO_2$) SBUs bridged with H_2TDC were designed.

On the other hand, because of the intrinsic high surface area-to-volume ratio and unique electronic and geometric structure, metal nanoclusters represent a novel class of highly efficient catalysts.[9−13] To date, much effort has been devoted to electrochemical water splitting to acquire clean hydrogen resources.[14,15] To this end, various catalysts have been developed for hydrogen evolution reaction.[16] Although Pt-based nanomaterials are the most efficient catalysts for hydrogen evolution reaction (HER),[17] the limited reserve in nature, high cost of Pt and the strong tendency to aggregate largely block the application of Pt NPs. One solution is to design an effective support for stabilizing Pt NPs while lowering the dosage of Pt and improving its atomic utilization.[18]

Here, we present a discrete trigonal prismatic coordination cage $\{Ni_{24}(TC4A\text{-}SO_2)_6(TDC)_{12}(H_2O)_6\}$ (**CIAC-121**) constructed by bridging the Ni_4-($TC4A\text{-}SO_2$) SBUs with TDC. Meanwhile, the prepared **CIAC-121** with small-sized cage, sulfur-containing framework and open structure provides a perfect environment for the formation and catalytic application of Pt NCs (Scheme 1). Electrochemical tests indicated that the synthesized Pt NCs have high electrocatalytic performance toward HER with low overpotential and high current density. The high catalytic activity could be attributed to the highly active surface of the ultrafine Pt NCs and the synergistic effect

Scheme 1. Illustration of the Assembly of Trigonal Prismatic $\{Ni_{24}\}$ Coordination Cage (CIAC-121) and the Fabrication of Ultrafine Pt NCs

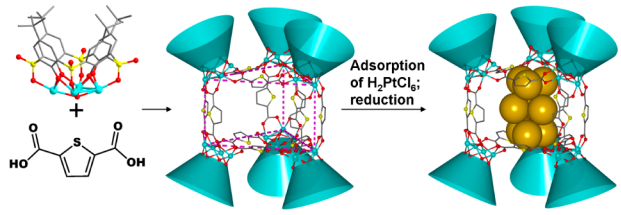

Received: October 27, 2016
Published: December 8, 2016

DOI: 10.1021/jacs.6b11218
J. Am. Chem. Soc. 2016, 138, 16236−16239

of the Pt NCs and the cage matrix. To our knowledge, this is one of the most efficient electrocatalysts for HER so far.

Compound **CIAC-121** was synthesized by a solvothermal reaction of H_4TC4A-SO_2, $NiCl_2 \cdot 6H_2O$ and H_2TDC under a basic condition. It crystallizes in the hexagonal system with space group $P\bar{6}m2$. The structure is featured by a nanosized trigonal prismatic coordination cage of calixarene (Figure 1 and

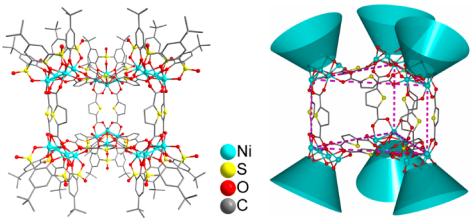

Figure 1. Crystal structure of a $\{Ni_{24}\}$ coordination cage in **CIAC-121**. Cyan truncated cones denote Ni_4-(TC4A-SO_2) SBUs and violet dotted lines represent the trigonal prismatic assembly.

S1). There are three crystallographically independent nickel sites (Ni1−Ni3) that are six-coordinated by two phenoxo μ_2-O atoms, one axial sulfonyl oxygen atom, one μ_4-oxygen and two carboxyl oxygen atoms from different TDC ligands, resulting in an approximately octahedral coordination environment. Analysis of the bond lengths and bond valence sum calculations suggest all nickel cations to be divalent. Four adjacent nickel atoms bond a calixarene molecule adopting a cone conformation to form a shuttlecock-like Ni_4-(TC4A-SO_2) SBU, whose bottom is capped by a μ_4-OH_2 molecule. Three such Ni_4-(TC4A-SO_2) SBUs are bridged by three TDC ligands into a coordination triangular framework which are further pillared by three pairs of TDC ligands to form a trigonal prism. Thus, six Ni_4-(TC4A-SO_2) SBUs are interconnected by 12 TDC linkers into an isolated trigonal prismatic $\{Ni_{24}\}$ coordination cage (Figures S1 and S2). So, there are 12 sulfur atoms on the surface of the cage cavity. The internal cavity is communicating to the outside through five apertures on the side facets and two bases. However, the communication between the internal void and the well-known calixarene cavity is blocked by the μ_4-OH_2 molecule at the bottom of the SBU. The nanocage has an inner cavity of about 12.1 × 12.1 × 9.6 Å measured between opposite μ_4-oxygen atoms of the coordinated water molecules. The discrete nanocages are stacked through molecular interactions into a 3D supramolecular structure with some hexagonal channels (Figure S3). The interstices are presumably occupied by some disordered solvent and organic amine molecules.

Under the similar reaction conditions, the analogous trigonal prismatic $\{Co_{24}\}$ coordination cage was not obtained. Instead, an isolated triangular $\{Co_{12}\}$ frame (**CIAC-122**) was obtained. **CIAC-122** crystallizes in the monoclinic system with space group $C2/c$. Different from those in **CIAC-121**, the shuttlecock-like Co_4-(TC4A-SO_2) SBUs are interconnected together by three pair of TDC ligands (Figures S4 and S5). The formation of different **CIAC-121** and **CIAC-122** would be due to different coordinaiton of nickel and cobalt.

In this work, a simple one-step method was designed to prepare the **Pt@CIAC-121** hybrid without any auxiliary reagents. As shown in Figure 2c, the MALDI-TOF MS spectra of **CIAC-121** give a sharp peak at 8814.0, which can be assigned to the species $[Ni_{24}(TC4A\text{-}SO_2)_6(TDC)_{12}(H_2O)_6] \cdot [(CH_3)_4N^+Cl^-] \cdot [(CH_3)_4N]^+$. After Pt NCs loading, three

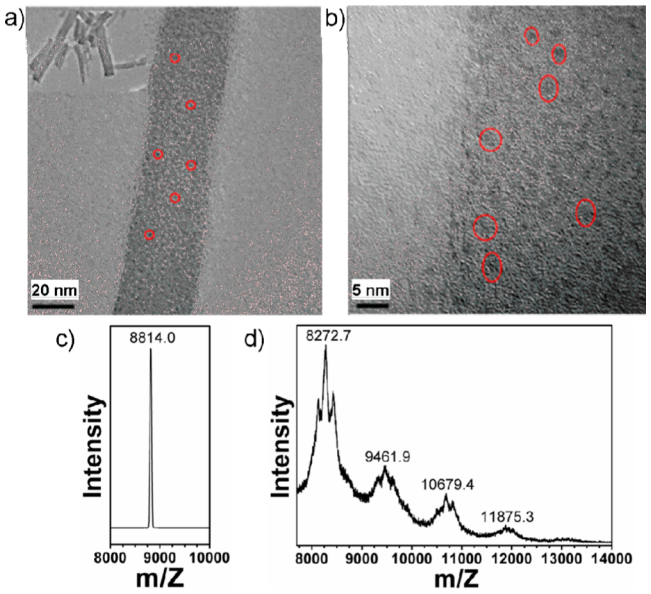

Figure 2. TEM images of the prepared **Pt@CIAC-121** hybrids at different magnifications (a, b) and MALDI mass spectra of **CIAC-121** before (c) and after Pt NCs loading (d). The scale bars are 20 nm (a) and 5 nm (b), respectively. The inset in panel a shows the morphology of the **Pt@CIAC-121** composite, which is similar to the original **CIAC-121**.

groups of peaks around 9461.9, 10 679.4 and 11 875.3 appeared, which would be assigned to the composites encapsulating Pt_6, Pt_{12} and Pt_{18}, respectively. During the reaction, **CIAC-121** plays three key roles for the formation of Pt NCs, i.e, reducing agent, stabilizing ligand and robust template. Briefly, because of the strong interaction between platinum and sulfur, which is demonstrated by the absorption of Pt−S bond at 328 cm^{-1} in the far IR spectrum (Figure S11),[19] the introduced ionic Pt species were initially sequestered into the cage of **CIAC-121**. Then, Pt(IV) species were gradually reduced to Pt(0) atoms through the electron transfer between metal and the surrounding organic groups of **CIAC-121**. Note that, similar to the previous reports, the ligands of H_2TDC and thiophene in the present study can serve as reducing agents for the formation of Pt clusters.[20] The formed Pt(0) atoms spontaneously collapsed and grew into Pt NCs. Because of the limited space of **CIAC-121** cage, only tiny Pt nanoclusters but not large Pt nanoparticles can be produced. Moreover, here we present a facile, straightforward and mild method compared to the reported methods for synthesis of metal@MOF and/or Mx(SR)y NCs.[21]

As shown in Figure S12, the original **CIAC-121** and **Pt@CIAC-121** hybrids show similar UV−vis absorption profiles with two peaks around 280 and 345 nm, indicating the stable structure of **CIAC-121** during encapsulating Pt NCs. However, a slight blue-shift from 349 to 344 nm and a new shoulder peak from 360 to 400 nm can be observed in the spectrum of **Pt@CIAC-121**, suggesting the possible electronic interaction between **CIAC-121** and Pt NCs. From the TEM measurements (Figure 2), ultrafine Pt nanoclusters have been successfully formed and evenly encapsulated in **CIAC-121** cage without changing the apparent cuboid morphology of **CIAC-121** crystals, indicating the structural robustness of **CIAC-121** (Figure 2a and inset). The average size of the formed Pt NCs was measured to be around 1.4 nm, close to the cage size of **CIAC-121**. In addition, the ICP-MS measurements further

DOI: 10.1021/jacs.6b11218
J. Am. Chem. Soc. 2016, 138, 16236−16239

demonstrated the formation of Pt species in the crystal of **CIAC-121** (Ni:Pt = 2.27:1). Supposing one cluster occupies one cage, the present Pt NC was calculated to be composed of 11 atoms, i.e., Pt_{11}, which is consistent with the results of MALDI-TOF MS.

The electrocatalytic performance of **Pt@CIAC-121** for HER was examined in 0.5 M H_2SO_4 and compared with Pt/C. As shown in Figure 3a, the **Pt@CIAC-121** shows an onset

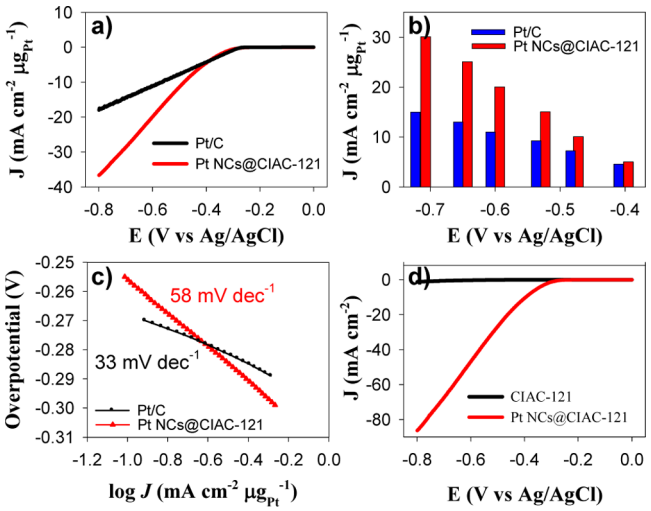

Figure 3. (a) Polarization curves of the **Pt@CIAC-121** and Pt/C for HER in 0.5 M H_2SO_4, with a potential scan rate of 50 mV/s. (b) Comparison of current densities from **Pt@CIAC-121** and Pt/C at different potentials. (c) Tafel plots from **Pt@CIAC-121** and Pt/C. (d) Polarization curves from **Pt@CIAC-121** and the parent **CIAC-121**.

potential of −0.24 V for HER, which is a little positive than that on Pt/C (−0.26 V). Meanwhile, the current density on **Pt@CIAC-121** is obviously larger than that obtained from Pt/C. Moreover, current densities of 5, 10, 15 and 20 mA·cm^{-2} μg^{-1} were obtained from the **Pt@CIAC-121** at the potentials of −0.40, −0.48, −0.53 and −0.60 V, respectively, which are around 1.1, 1.38, 1.6 and 2.0 times higher than those from Pt/C (Figure 3b). These results suggest that the **Pt@CIAC-121** hybrid has enhanced electrocatalytic performance for HER and thus the usage of Pt can be largely reduced. Moreover, with respect to the onset potential and current density, the present **Pt@CIAC-121** shows much better performance than the reported noble metal-based electrocatalysts for HER.[17a,22] The electrochemical stability of the **Pt@CIAC-121** was also evaluated by accelerated durability tests (ADTs). As shown in Figure S13, after 5000 cycles tests, the HER current density from the **Pt@CIAC-121** is still much higher than that from Pt/C. Such a result indicates the higher durability and stronger corrosion-resistance of the **Pt@CIAC-121** compared to the Pt/C.

For comparison, **CIAC-122**, H_4TC4A-SO_2 and the mixture of H_4TC4A-SO_2 and H_2TDC were also used to synthesize Pt NCs. As shown in Figure S14, similar Pt NCs can be formed in the **CIAC-122** frames. However, only large Pt NPs were produced with the mixture of H_4TC4A-SO_2 and H_2TDC, and no Pt NCs or NPs can be observed with H_4TC4A-SO_2 (Figure S15). The electrochemical measurements shown in Figure S16 indicate that the **Pt@CIAC-121** has the highest electrocatalytic activity for HER.

To get the mechanistic insights into the outstanding catalytic activity of **Pt@CIAC-121** for HER, catalytic kinetic was evaluated from the Tafel plots (Figure 3c). The Tafel slope of 58 mV·dec^{-1} from the **Pt@CIAC-121** reveals that the rate-determining step of HER is the electrochemical desorption process, i.e., the Heyrovsky reaction. In comparison, the Tafel slope of 33 mV·dec^{-1} from commercial Pt/C suggests that the Tafel recombination step is the dominated process.[23] These results show that two different mechanisms are involved in these two catalysts. As shown in Figure 3d, compared to **Pt@CIAC-121**, the current density from pure **CIAC-121** is negligible, indicating that the catalytic activity of **Pt@CIAC-121** is mainly from the encapsulated Pt NCs.

In addition, XPS was performed to get further insight into the high catalytic activity of **Pt@CIAC-121** (Figure S17). The deconvoluted XPS of Pt 4f displays two sets of peaks (Figure 4a), corresponding to the Pt^0 and Pt^{2+}, respectively, further

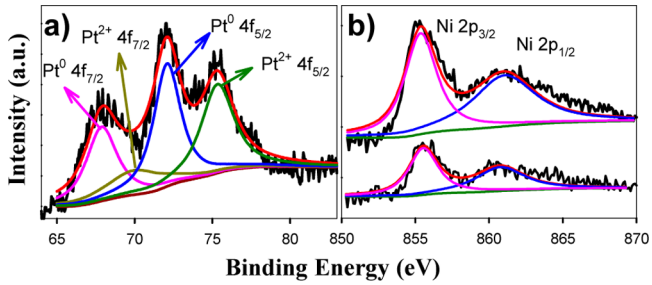

Figure 4. (a) Deconvoluted Pt 4f XPS of the **Pt@CIAC-121**; (b) deconvoluted XPS spectra of Ni in **Pt@CIAC-121** (top) and **CIAC-121** (bottom).

demonstrating the successful encapsulation of Pt NCs in **CIAC-121** cages. Interestingly, compared to the original **CIAC-121**, the Ni 2p binding energy from the **Pt@CIAC-121** shows an obvious upshift (Figure 4b), indicating that nickel ions centers are electron donators in the hybrid system, which can increase the electron density of the Pt NC and in turn enhance the electrocatalytic activity for HER. Moreover, the binding energy of S 2p in **Pt NC@CIAC-121** shows an obvious shift compared to that in **CIAC-121** (Figure S18), suggesting again the interaction between Pt and S.

In summary, we present a novel calixarene-based trigonal prismatic coordination cage, constructed by six Ni_4-(TC4A-SO_2) SBUs as vertices and 12 TDC ligands as arris. Based on the strong covalent interaction between Pt and sulfur, ultrafine Pt NCs were confined inside the coordination cages. The Pt NCs exhibited high electrocatalytic activity for HER with an onset potential of −0.24 V and current density of 10 mA·cm^{-2}·μg^{-1} Pt at the potential of −0.48 V, which are much superior to those from Pt/C. The present study not only demonstrates a novel coordination cage structure but also provides a method for synthesizing confined metal nanoclusters with promising application in catalysis.

■ ASSOCIATED CONTENT

Supporting Information

The Supporting Information is available free of charge on the ACS Publications website at DOI: 10.1021/jacs.6b11218.

Experimental section, single-crystal structure determination, other figures and detailed analyses (PDF)
Data for **CIAC-121** (CIF)

DOI: 10.1021/jacs.6b11218
J. Am. Chem. Soc. 2016, 138, 16236−16239

Data for **CIAC-122** (CIF)

AUTHOR INFORMATION

Corresponding Authors

*W.L. wpliao@ciac.ac.cn

*W.C. weichen@ciac.ac.cn

ORCID

Wuping Liao: 0000-0001-8209-6189

Author Contributions

S.W. and X.G. contributed equally.

Notes

The authors declare no competing financial interest.

ACKNOWLEDGMENTS

This work was supported by National Natural Science Foundation of China (Nos. 21571172, 21521092, 21633008, 21575134, and 51222404) and National Key Research and Development Plan (2016YFA0203200).

REFERENCES

(1) (a) Cook, T. R.; Stang, P. J. *Chem. Rev.* **2015**, *115*, 7001. (b) Cook, T. R.; Zheng, Y. R.; Stang, P. J. *Chem. Rev.* **2013**, *113*, 734. (c) Zarra, S.; Wood, D. M.; Roberts, D. A.; Nitschke, J. R. *Chem. Soc. Rev.* **2015**, *44*, 419. (d) Ward, M. D.; Raithby, P. R. *Chem. Soc. Rev.* **2013**, *42*, 1619.

(2) (a) Lu, Z.; Knobler, C. B.; Furukawa, H.; Wang, B.; Liu, G.; Yaghi, O. M. *J. Am. Chem. Soc.* **2009**, *131*, 12532. (b) Li, J. R.; Zhou, H. C. *Nat. Chem.* **2010**, *2*, 893. (c) Ballester, P.; Fujita, M.; Rebek, J., Jr *Chem. Soc. Rev.* **2015**, *44*, 392.

(3) (a) McConnell, A. J.; Wood, C. S.; Neelakandan, P. P.; Nitschke, J. R. *Chem. Rev.* **2015**, *115*, 7729. (b) Vardhan, H.; Yusubov, M.; Verpoort, F. *Coord. Chem. Rev.* **2016**, *306*, 171. (c) Brown, C. J.; Toste, F. D.; Bergman, R. G.; Raymond, K. N. *Chem. Rev.* **2015**, *115*, 3012.

(4) (a) Chen, Y. Z.; Zhou, Y. X.; Wang, H. W.; Lu, J. L.; Uchida, T.; Xu, Q.; Yu, S. H.; Jiang, H. L. *ACS Catal.* **2015**, *5*, 2062. (b) Guo, Z.; Xiao, C.; Maligal-Ganesh, R. V.; Zhou, L.; Goh, T. W.; Li, X.; Tesfagaber, D.; Thiel, A.; Huang, W. *ACS Catal.* **2014**, *4*, 1340.

(5) Dalgarno, S. J.; Thallapally, P. K.; Barbour, L. J.; Atwood, J. L. *Chem. Soc. Rev.* **2007**, *36*, 236.

(6) Liu, M.; Liao, W. P.; Hu, C. H.; Du, S. C.; Zhang, H. J. *Angew. Chem., Int. Ed.* **2012**, *51*, 1585.

(7) Hang, X. X.; Liu, B.; Zhu, X. F.; Wang, S. T.; Han, H. T.; Liao, W. P.; Liu, Y. L.; Hu, C. H. *J. Am. Chem. Soc.* **2016**, *138*, 2969.

(8) (a) Xiong, K. C.; Jiang, F. L.; Gai, Y. L.; Yuan, D. Q.; Chen, L.; Wu, M. Y.; Su, K. Z.; Hong, M. C. *Chem. Sci.* **2012**, *3*, 2321. (b) Dai, F. R.; Wang, Z. Q. *J. Am. Chem. Soc.* **2012**, *134*, 8002. (c) Su, K. Z.; Jiang, F. L.; Qian, J. J.; Chen, L.; Pang, J. D.; Bawaked, S. M.; Mokhtar, M.; Al-Thabaiti, S. A.; Hong, M. C. *Inorg. Chem.* **2015**, *54*, 3183.

(9) (a) Qian, H.; Zhu, M.; Wu, Z.; Jin, R. *Acc. Chem. Res.* **2012**, *45*, 1470. (b) Yao, Q.; Yuan, X.; Yu, Y.; Xie, J.; Lee, J. Y. *J. Am. Chem. Soc.* **2015**, *137*, 2128.

(10) (a) Lee, L. C.; Zhao, Y. *ACS Catal.* **2014**, *4*, 688. (b) Zhu, Y.; Qian, H. F.; Drake, B. A.; Jin, R. C. *Angew. Chem., Int. Ed.* **2010**, *49*, 1295. (c) Yoskamtorn, T.; Yamazoe, S.; Takahata, R.; Nishigaki, J.; Thivasasith, A.; Limtrakul, J.; Tsukuda, T. *ACS Catal.* **2014**, *4*, 3696.

(11) (a) Nie, X. T.; Qian, H. F.; Ge, Q. J.; Xu, H. Y.; Jin, R. C. *ACS Nano* **2012**, *6*, 6014. (b) Manzoor, D.; Pal, S. *J. Phys. Chem. C* **2014**, *118*, 30057.

(12) Gao, X.; Du, C.; Zhang, C.; Chen, W. *ChemElectroChem* **2016**, *3*, 1266.

(13) Vilar-Vidal, N.; Rivas, J.; Lopez-Quintela, M. A. *ACS Catal.* **2012**, *2*, 1693.

(14) Li, Y. G.; Wang, H. L.; Xie, L. M.; Liang, Y. Y.; Hong, G. S.; Dai, H. J. *J. Am. Chem. Soc.* **2011**, *133*, 7296.

(15) Popczun, E. J.; McKone, J. R.; Read, C. G.; Biacchi, A. J.; Wiltrout, A. M.; Lewis, N. S.; Schaak, R. E. *J. Am. Chem. Soc.* **2013**, *135*, 9267.

(16) (a) Xiao, P.; Sk, M. A.; Thia, L.; Ge, X. M.; Lim, R. J.; Wang, J. Y.; Lim, K. H.; Wang, X. *Energy Environ. Sci.* **2014**, *7*, 2624. (b) Cao, B. F.; Veith, G. M.; Neuefeind, J. C.; Adzic, R. R.; Khalifah, P. G. *J. Am. Chem. Soc.* **2013**, *135*, 19186. (c) Zou, X. X.; Huang, X. X.; Goswami, A.; Silva, R.; Sathe, B. R.; Mikmekova, E.; Asefa, T. *Angew. Chem., Int. Ed.* **2014**, *53*, 4372.

(17) (a) Fan, Z. X.; Luo, Z. M.; Huang, X.; Li, B.; Chen, Y.; Wang, J.; Hu, Y. L.; Zhang, H. *J. Am. Chem. Soc.* **2016**, *138*, 1414. (b) Hsu, I. J.; Kimmel, Y. C.; Jiang, X. G.; Willis, B. G.; Chen, J. G. *Chem. Commun.* **2012**, *48*, 1063. (c) Popczun, E. J.; Read, C. G.; Roske, C. W.; Lewis, N. S.; Schaak, R. E. *Angew. Chem., Int. Ed.* **2014**, *53*, 5427.

(18) (a) Esposito, D. V.; Hunt, S. T.; Stottlemyer, A. L.; Dobson, K. D.; McCandless, B. E.; Birkmire, R. W.; Chen, J. G. G. *Angew. Chem., Int. Ed.* **2010**, *49*, 9859. (b) Grigoriev, S. A.; Millet, P.; Fateev, V. N. *J. Power Sources* **2008**, *177*, 281.

(19) Kang, X.; Xiong, L.; Wang, S.; Yu, H.; Jin, S.; Song, Y.; Chen, T.; Zheng, L.; Pan, C.; Pei, Y.; Zhu, M. *Chem. - Eur. J.* **2016**, *22*, 17145.

(20) Bae, S. E.; Kim, K. J.; Hwang, Y. K.; Huh, S. *J. Colloid Interface Sci.* **2015**, *456*, 93.

(21) (a) Hu, P.; Morabito, J. V.; Tsung, C. K. *ACS Catal.* **2014**, *4*, 4409. (b) Aijaz, A.; Karkamkar, A.; Choi, Y. J.; Tsumori, N.; Ronnebro, E.; Autrey, T.; Shioyama, H.; Xu, Q. *J. Am. Chem. Soc.* **2012**, *134*, 13926. (c) Wang, H. K.; Chen, F. Y.; Li, W. Y.; Tian, T. *J. Power Sources* **2015**, *287*, 150.

(22) Wu, M.; Shen, P. K.; Wei, Z. D.; Song, S. Q.; Nie, M. *J. Power Sources* **2007**, *166*, 310.

(23) Chen, W. F.; Muckerman, J. T.; Fujita, E. *Chem. Commun.* **2013**, *49*, 8896.

DOI: 10.1021/jacs.6b11218
J. Am. Chem. Soc. 2016, 138, 16236−16239